Synthesis, Biological Activity, and Conformational Analysis of Peptidomimetic Analogues of the *Saccharomyces cerevisiae* α-Factor Tridecapeptide†

Y. Larry Zhang,‡ Hanumantha Rao Marepalli,‡ Hui-fen Lu,§ Jeffrey M. Becker,*,§ and Fred Naider‡

Department of Chemistry, The College of Staten Island and The Graduate School of The City University of New York, Staten Island, New York 10314, and Department of Microbiology and Department of Biochemistry, Cellular and Molecular Biology, University of Tennessee, Knoxville, Tennessee 37996

Received April 8, 1998; Revised Manuscript Received July 13, 1998

ABSTRACT: Biochemical and biophysical investigations on the *Saccharomyces cerevisiae* α-factor indicate that this tridecapeptide mating pheromone (WHWLQLKPGQPMY) might adopt a type II β-turn in the center of the peptide when it binds to its G protein-coupled receptor. To test this hypothesis we synthesized analogues of α-factor incorporating a (*R* or *S*)-γ-lactam conformational constraint [3-(*R* or *S*)-amino-2-oxo-1-pyrrolidineacetamido] in place of the Pro-Gly at residues 8 and 9 of the peptide and tested their biological activities and receptor binding. Analogues were purified to >99% homogeneity as evidenced by high-performance liquid chromatography and capillary electrophoresis and characterized by amino acid analysis, mass spectrometry, and nuclear magnetic resonance (NMR) spectroscopy. The restricted α-factor analogue WHWLQLK[(*R*)-γ-lactam]QP[Nle]Y was more active than its lactam-containing diastereomeric homologue WHWLQLK[(*S*)-γ-lactam]QP[Nle]Y and about equally active with the [Nle^{12}]-α-factor in growth arrest and *FUS1*−*lacZ* gene induction assays. Both lactam analogues competed with tritiated [Nle^{12}]-α-factor for binding to the α-factor receptor (Ste2p) with the (*R*)-γ-lactam-containing peptide having 7-fold higher affinity than the (*S*)-γ-lactam-containing homologue. Two-dimensional NMR spectroscopy and modeling analysis gave evidence that the (*R*)-γ-analogue is a flexible peptide that assumes a transient γ-turn structure around the lactam moiety. The results represent the first example of an α-factor analogue containing a peptidomimetic constraint that is as active as the native pheromone. The correlation between activity and structure provides further evidence that the biologically active conformation of the molecule contains a turn in the middle of the pheromone. This study provides new insights into the structural basis of α-factor activity and adds to the repertoire of conformationally biasing constraints that can be used to maintain and even enhance biological activity in peptide hormones.

Sexual reproduction of the yeast *Saccharomyces cerevisiae* is triggered by reciprocal pheromonal exchange between cells of the opposite mating types *MAT*α and *MAT***a** (for review, see ref *1*). The pheromones have been identified as peptides: α-factor [WHWLQLKPGQPMY] secreted by *MAT*α cells (*2*) and **a**-factor [YIIKGVFWDPAC(s-farnesyl)-OCH_3] secreted by *MAT***a** cells (*3*). As is true of many peptide hormones in vertebrate tissues, these two pheromones are recognized by G protein-coupled receptors on the surface of the target cells (*4,* 5). Signal transduction is thought to be initiated through a conformational change of the receptor protein that is induced by ligand binding. This isomerization subsequently influences the interaction between the receptor molecule and the heterotrimeric G protein, ultimately resulting in the triggering of a cascade of intracellular events (*6*). The mating process in the unicellular eukaryotic *S. cerevisiae* provides a powerful paradigm to study the molecular basis for G protein-coupled, receptor-mediated signal transduction (*1*).

Biochemical and biophysical analyses on α-factor and its analogues have provided evidence that a β-turn involving the Pro^8-Gly^9 residues might be an important determinant of the biologically active structure of the pheromone (*7,* 8). Thus, replacing Gly with D-Ala at position 9 of α-factor resulted in an agonist with biological activity 4−5-fold higher than that of the natural pheromone, while in contrast, the [L-Ala^9]-α-factor was 10-fold less active. Conformational analysis of such analogues indicated that in organic and aqueous solutions the [D-Ala^9]-α-factor assumed a transient type II β-turn whereas the [L-Ala^9]-α-factor was not structured. Efforts directed toward enhancing this presumed secondary structural motif by cyclization of the side-chain residues 7−10 have so far not succeeded in generating an agonist with bioactivity equal to, or better than, that of the wild-type pheromone (*9*−*12*).

A recent systematic investigation of the importance of the side-chain functionality and orientation in α-factor showed that replacing Lys^7 or Gln^{10} with L-Ala yielded analogues that were a half and a third as active as α-factor, respectively (*13*). D-Ala replacement at these two positions gave a ninth and less than a hundredth the bioactivity of α-factor,

† This work was supported by NIH Grants GM-22086 and GM-22087. The CUNY College of Staten Island NMR facility is funded by NSF Grant BIR-9214560, The City University of New York, and The New York State Higher Education Advanced Technology Program.

* Corresponding author: Tel (423) 974-3006; Fax (423) 974-4007; e-mail jbecker@utk.edu.

‡ The College of Staten Island and The Graduate School of The City University of New York.

§ University of Tennessee.

S0006-2960(98)00787-9 CCC: $15.00
Published on Web 08/20/1998

respectively, and a 3-order magnitude drop in receptor affinity. These findings stress the importance of the side-chain orientations at positions 7 and 10 and thus suggest that approaches other than covalent bond formation between these side chains may be necessary to conformationally restrict the central turn region of α-factor.

Studies aimed at enhancing the natural propensities of residues in biologically active peptides to assume specific turns have been extensively undertaken since the 1970s. Most of the reported efforts focused on modifying the central portion (residues $i + 1$ and/or $i + 2$) of β-turn regions while leaving the rest of the peptide intact. Compared with the other turn mimetics [e.g., bicyclic dipeptide BTD (*14*), proline derivatives (*15*), and spirolactam bicyclic and tricyclic systems (*16, 17*)], Freidinger's γ-lactam-constrained dipeptide building blocks seem quite attractive for the following reasons: (i) they have been successfully incorporated into LHRH[1] to covalently restrict a putative type II′ β-turn secondary structure (*18*); (ii) some spectroscopic investigations have been reported to support the restricted dihedral angle(s) (*19, 20*); (iii) a similar constraint, α-aminosuccinimide, has been found as a naturally existing motif in human growth hormone (*21*); and (iv) a convenient synthetic procedure was developed to incorporate the γ-lactam constrained dipeptide into linear peptides during solid-state synthesis (*22*). Recently, theoretical calculations suggested that simple substitution of Pro-D-NMe-AA or D-Pro-NMe-AA (where AA = amino acid other than Gly) into a peptide sequence stabilizes a β-turn as well (*23*).

In this paper we report the synthesis and biological activity of constrained analogues of α-factor using the Freidinger's γ-lactam peptidomimetic to alter the conformation of the center of the peptide (Figure 1). We have also synthesized and determined the biological activity of several α-factor analogues with substitutions predicted to have a stabilizing effect on the β-turn of peptides (*23*). Circular dichroism, two-dimensional NMR, and computer modeling were used to assess the structure of [(*R*)-γ-lactam^{8,9}, Nle^{12}]-α-factor (**4**; Figure 1), the pheromone peptidomimetic with the highest biological activity. Our results indicate that the incorporation of Freidinger's (*R*)-γ-lactam in the center of α-factor results in the first peptidomimetic pheromone that is equally active to α-factor. Moreover, the conformational studies are consistent with the conclusion that analogues of α-factor with turns in the middle of the pheromone can bind to the receptor and efficiently trigger signal transduction.

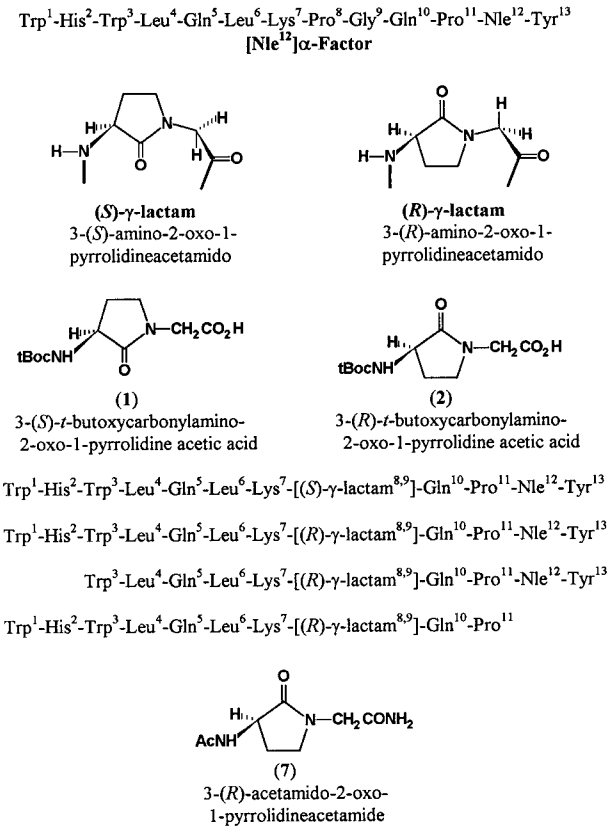

FIGURE 1: Primary structure of Freidinger's γ-lactams and lactam-containing α-factor analogues.

EXPERIMENTAL PROCEDURES

Synthesis of γ-Lactam Peptidomimetic Building Blocks. The γ-lactam building blocks, 3-(*S*)-(*tert*-butoxycarbonyl)-amino-2-oxo-1-pyrrolidineacetic acid **(1)** and 3-(*R*)-(*tert*-butoxycarbonyl)amino-2-oxo-1-pyrrolidineacetic acid **(2)**, were synthesized by a modification of the procedures of Freidinger et al. (*22*). Predried Boc-Met-Gly-OMe methylsulfonium iodide or Boc-D-Met-Gly-OMe methylsulfonium iodide (5 mmol) was dissolved in a predried 1:1 mixture of DCM and DMF (60 mL) and cooled to 0 °C. Sodium hydride (powder, 11 mmol) was added in one portion to the stirred solution under nitrogen and the reaction was allowed to continue at 0 °C for 2.5 h. Methyl acetate (30 mL) and water (8 mL) were added and the resulting solution was left overnight at room temperature. Solvents were removed under vacuum and the residue was partitioned between water (50 mL) and DCM (50 mL). The pH was then adjusted to 12 with 1 M NaOH under vigorous stirring at room temperature for 5 min to hydrolyze methyl 3-(*R or S*)-(*tert*-butoxycarbonyl)amino-2-oxo-1-pyrrolidineacetate. The pH was lowered to 8.5 with 1 M HCl and the aqueous layer was washed with DCM (3 × 50 mL). The aqueous layer was further acidified to pH 2.5 with 1 M HCl in the presence of ethyl acetate and saturated with sodium chloride. Additional extractions with ethyl acetate (4 × 50 mL) were carried out, and the ethyl acetate layers were combined, washed with brine (2 × 20 mL) and water (1 × 20 mL), and dried over magnesium sulfate for 2 h. Removal of solvent gave a white solid. Recrystallization in methanol−ethyl acetate−cyclohexane (1:19:80 v/v/v) resulted in greater than 98% pure product (**1** or **2**). ^{1}H NMR of **1** or **2** in

[1] Abbreviations: 2D NMR, two-dimensional nuclear magnetic resonance; Ac, acetyl; Boc, *tert*-butoxycarbonyl; BrZ, (2-bromobenzyl)-oxycarbonyl; Bu, butyl; CD, circular dichroism; DCM, dichloromethane; DIEA, diisopropylethylamine; DIPC, diisopropylcarbodiimide; DMF, *N*,*N*-dimethylformamide; DMS, dimethyl sulfide; DMSO, dimethyl sulfoxide; DQF-COSY, double quantum filtered correlation spectroscopy; FAB-MS, fast atom bombardment mass spectroscopy; Fmoc, 9-fluorenylmethoxycarbonyl; For, formyl; HMQC, heteronuclear multiple-quantum coherence; HOBt, 1-hydroxybenzotriazole; HPLC, high-performance liquid chromatography; LHRH, luteinizing hormone-releasing hormone; MBHA, 4-methylbenzhydrylamine; MD, molecular dynamics; Nle, l-norleucyl; NOE, nuclear Overhauser effect; NOESY, nuclear Overhauser effect spectroscopy; PAM, [(4-hydroxymethyl)-phenyl]acetamidomethyl; tBu, *tert*-butyl; TFA, trifluoroacetic acid; TMS, tetramethylsilane; TOCSY, total correlation spectroscopy; Wang resin, (4-hydroxymethyl)phenoxymethyl on 1% cross-linked polystyrene resin (bead); YEPD, a mixture of yeast extract (1%), peptone (2%), and dextrose (2%); Z, benzyloxycarbonyl.

DMSO-d_6: δ 12.9 (br s, 1 H), 7.10 (d, 1 H), 4.10 (m, 1 H), 3.95 (m, 2 H), 3.30 (m, 2 H), 2.3 (m, 1 H), 1.85 (m, 1 H), and 1.37 (s, 9 H).

Synthesis of 3-(R)-Acetamido-2-oxo-1-pyrrolidineacetamide (7). MBHA resin (Bachem; 0.5 mmol) was swelled in DCM and coupled with 3-(*R*)-(*tert*-butoxycarbonyl)amino-2-oxo-1-pyrrolidineacetic acid (**2**) (1 mmol) in the presence of DIPC (1 mmol) and HOBt (1 mmol) in DCM at room temperature for 24 h. The resulting resin was washed with DMF (3×) and DCM (5×). Boc deprotection was carried out in 45% TFA in DCM containing 2% DMS at room temperature for 30 min. The resin was washed with DCM (5×), treated with 5% DIEA in DCM, and washed with DCM (3×) and DMF (5×). *N*-Acetylation was performed at room temperature in DMF using acetic anhydride (10 mmol) and DIEA (10 mmol) for 30 min. After being washed with DMF (3×), DCM (5×), and methanol (3×), the resin was dried in vacuo overnight. The product was released from the resin by HF treatment in the presence of anisole (10%) at 0 °C for 1 h, precipitated, and washed with ethyl ether. The crude product was dissolved in water and lyophilized to a yellow oil. Purification was carried out by reversed-phase HPLC on a semipreparative Waters μBondapak C_{18} column (19 mm × 300 mm) with elution by 100% water. The fractions of over 98% homogeneity were combined and lyophilized to give a white solid (>85% overall yield). FAB-MS $[M + 1]^+$: calculated, 200.2; found, 200.1. ^{1}H NMR of **7** in DMSO-d_6: δ 8.25 (d, 1 H), 7.36 (s, 1 H), 7.14 (s, 1 H), 4.33 (m, 1 H), 3.98 (dd, 1 H), 3.90 (dd, 1 H), 3.33 (m, 2 H), 2.29 (m, 1 H), 1.83 (s, 3 H), and 1.79 (m, 1 H).

Peptide Synthesis and Purification. The solid-phase syntheses of all γ-lactam-containing α-factors were carried out manually, starting with *N*-α-Boc-Tyr(2-BrZ)-PAM resin. *tert*-Butoxycarbonyl was employed for all *N*-α protections while the side-chain protecting groups were Trp (For), His (Tos), and Lys (Cl-Z). All analogues with substitutions in position 9 were synthesized by automated solid-phase techniques using Fmoc chemistry. Details of these procedures were reported previously (*9*, *11*−*13*). The yields of the crude peptides after cleavage from the resin and lyophilization were about 60−80% as judged by analytical HPLC. The crude peptides were purified by reversed-phase HPLC (Hewlett-Packard Series 1050) on a semipreparative Waters μBondapak C_{18} column (19 mm × 300 mm) as previously described. The homogeneity of the purified peptide was judged by analytical HPLC using two different solvent systems (acetonitrile−water and methanol−water) and capillary electrophoresis (Hewlett-Packard 3D-CE Model G1600A) using a Hewlett-Packard fused silica capillary (L = 56 cm, i.d. = 50 μm) at 30 kV and pH 2.5 (0.1 M sodium phosphate buffer). Amino acid analysis was carried out at Brigham and Women's Hospital, Boston, MA. FAB-mass spectrometry was done at the University of Tennessee, Knoxville, TN.

CD Spectroscopy. CD spectra of [(*R*)-γ-lactam^{8,9}, Nle^{12}]-α-factor (**4**), 3-(*R*)-acetamido-2-oxo-1-pyrrolidineacetamide (**7**), [Nle^{12}]-α-factor and equimolar mixtures of **7** and [Nle^{12}]-α-factor were recorded on a Jasco 500 spectropolarimeter at an ambient temperature (∼ 25 °C) using 0.05 cm path length circular quartz cells. Both the optics and chamber were flushed continuously with dry nitrogen throughout the experiment. The instrument was calibrated with an aqueous solution of d-(+)-10-camphorsulfonic acid at 290 nm. Tris buffer (50 mM, pH 7.2) was used to make peptide solutions. CD spectra were obtained for peptide solutions of 0.25, 0.50, and 1 mM concentrations. CD spectra over a wavelength range of 190−260 nm were recorded at a scan speed of 10 nm/min and a wavelength expansion of 10 nm/cm. All spectra were corrected by subtracting the solvent baseline recorded under identical conditions. The ellipticity is reported as molar ellipticity ($[\theta]_m$) in deg·cm^{2}dmol^{-1}, where the actual molecular weight of the peptide and not the mean residue molecular weight was used to calculate ellipticity (*24*). In the additivity experiment, for molar ellipticity calculations, the average concentration and a modified molecular weight (average molecular weight of the two peptides) were used.

NMR Spectroscopy. NMR spectra for 3-(*S*)-(*tert*-butoxycarbonyl)amino-2-oxo-1-pyrrolidineacetic acid (**1**), 3-(*R*)-(*tert*-butoxycarbonyl)amino-2-oxo-1-pyrrolidineacetic acid (**2**), [(*R*)-γ-lactam^{8,9}, Nle^{12}]-α-factor (**4**), and 3-(*R*)-acetamido-2-oxo-1-pyrrolidineacetamide (**7**) were acquired on a Varian Unityplus 600 MHz NMR spectrometer. Peptide **4**, predried in an Abderhalden drying pistol over refluxing methanol under high vacuum, and 100% DMSO-d_6 (Aldrich, Milwaukee, WI) were used to make 0.125, 0.25, 0.50, and 1 mM solutions. Proton and carbon chemical shifts were referenced against TMS and DMSO at 0 and 39.5 ppm, respectively. Conformational analysis of **4** was done on a 1 mM solution. One-dimensional proton NMR spectra were acquired at 295−325 K in increments of 5 K to determine temperature coefficients of amide protons.

Homo- and heteronuclear 2D NMR experiments were performed to assign ^{1}H and ^{13}C resonances. DQF-COSY (*25*, *26)*, TOCSY (*27*−*29*), NOESY (*30*), HMQC (*31*, *32*), and HMQC-TOCSY (*33*) were recorded in phase-sensitive mode using the hypercomplex method (*34*). The indirect detection heteronuclear multiple-quantum coherence experiments, HMQC and HMQC-TOCSY, were used to assign ^{13}C resonances. Two-dimensional NMR experiments were acquired with 2048 data points in t_2, for 512 t_1 increments with a relaxation delay of 2 s and 32 transients for each t_1 increment. The spectral width in homonuclear experiments in both dimensions was 7000 Hz, while in the heteronuclear experiments it was 7000 Hz in the t_2 dimension and 30 000 Hz in the t_1 dimension. A 9 kHz spin-lock field was employed both in TOCSY and in HMQC-TOCSY experiments. NOESY experiments with 100, 250, and 400 ms mixing time were recorded. NMR data were processed on a Sun Sparcstation IPX with VNMR software. Two-dimensional data were apodized using phase-shifted sine bell or Gaussian window functions and zero-filled to 2K × 2K.

Computational Procedures: Structure Buildup and Energy Minimization. To generate the α-factor analogue containing the γ-lactam moiety, the extended structure of [D-Met^8, Nle^{12}]-α-factor was first assembled with the BIOPOLYMER module of the SYBYL software on an Indigo2 SGI workstation. The S−CH_3 group of Met^8 and the amide N*H* of Gly^9 were removed and γ-lactam was generated by covalently linking the C_γ of Met^8 with the amide nitrogen of Gly^9. All energy minimizations were performed with the AMBER force field. Simplexing followed by a few cycles of steepest-descent minimization were carried out to normalize the bond angles and bond lengths in the cyclic portion of the peptide

Table 1: ^{1}H Assignments for [(*R*)-γ-Lactam^{8,9}, Nle^{12}]-α-factor (**4**) in DMSO-d_6[a]

residue	N*H*	$^{\alpha}$C*H*	$^{\beta}$C*H*	$^{\gamma}$C*H*	$^{\delta}$C*H*	$^{\epsilon}$C*H*	others
Trp^1		4.06	2.98, 3.13				ring protons 6.78, 7.00, 7.16, 7.32, 7.57, indole N*H* 10.94
His^2	8.90	4.68	3.04				C_2H 7.15, C_4H 7.18
Trp^3	8.27	4.63	2.99, 3.18				ring protons 6.98, 7.06, 7.18, 7.33, 7.68, indole N*H* 10.85
Leu^4	8.46	4.38	1.46	1.59	0.82, 0.87		
Gln^5	8.09	4.29	1.77, 1.87	2.12			γ-NH_2 6.84, 7.31
Leu^6	7.98	4.31	1.45	1.59	0.81, 0.84		
Lys^7	7.90	4.28	1.61	1.29	1.51	2.74	ε-N$^+H_3$ 7.67
γ-lac^8	8.36	4.29	1.77, 2.29	3.30			
Gly^9		3.82, 3.90					
Gln^{10}	8.23	4.46	1.70, 1.88	2.13			γ-NH_2 6.81, 7.30
Pro^{11}		4.36	1.84, 1.94	1.77	3.62		
Nle^{12}	7.89	4.20	1.45, 1.59	1.23	1.23	0.83	
Tyr^{13}	7.95	4.33	2.79, 2.90				$C_{3.5}H$ 6.63, $C_{2.6}H$ 6.98

[a] Chemical shifts are given in parts per million downfield from internal tetramethylsilane.

and relax the close contacts, if any, in the molecule. This was followed by Powell minimization. The lowest energy structure obtained in this manner was then subjected to constrained searches and minimizations using the annealing procedure in SYBYL (consecutive dynamics at $T = 500$ and 20 K). The results were analyzed and conformations compatible with the experimental data were identified and further searched and minimized. The NMR constraints were input as ranges centered on the experimentally determined distance (±10% of the distance value). Pseudoatom corrections were applied to those methylene proton pairs that were indistinguishable. Dihedral angles deduced from coupling constants were not used as constraints due to degeneracy but rather were used for evaluating the model obtained from NMR-derived distance constraints. The vacuum-minimized structure (closest to experimental constraints) was solvated with DMSO molecules (*35*) and minimized using the AMBER (Kollman all-atom) force field with periodic boundary conditions. The typical length of the parallelepipedic solvent box was between 34 and 44 Å and contained around 400 DMSO molecules.

Molecular Dynamics Simulations. Molecular dynamics (MD) simulations were performed on [(*R*)-γ-lactam^{8,9}, Nle^{12}]-α-factor (**4**) to evaluate the conformational flexibility of the molecule and to obtain an ensemble of structures. MD simulations were carried out with NOE-derived distance constraints both in a vacuum and in DMSO using the AMBER force field and *Verlet* algorithm. Simulations were initiated from well energy-minimized structures obtained in a vacuum and DMSO as explained above. The final temperature of 300 K was reached in three steps: heating at 1000 K for 3 ps, cooling to 500 K for 5 ps, equilibration at 300 K for 12 ps, and simulations at 300 K for 200 ps. Two thousand trajectories were generated by taking snapshots every 100 fs. The step size for the integration of Newton's equation was 1 fs for MD simulations both in a vacuum and in DMSO. The thermodynamic ensemble used was NTV. The rms deviations for each average distance in the ensemble of 2000 structures are presented in Table 2. As a control experiment, the NMR-compatible structure obtained from constrained searches and minimizations was subjected to further minimization without constraints and MD simulations were performed under similar conditions. Furthermore, MD simulations were also performed under identical conditions on the initial extended structure of [(*R*)-γ-lactam^{8,9}, Nle^{12}]-α-factor (**4**) (which was used as starting structure for constrained searches) to find out whether the covalent geometry of the lactam alone is able to induce the turn structure into the peptide.

Table 2: Comparison of Experimental and Modeling Interproton Distances for [(*R*)-γ-Lactam^{8,9}, Nle^{12}]-α-factor (**4**)

protons		NOESY cross- peak volume[a]	NOESY distance[a] (Å)	MD in DMSO Average (Å)[b]
Trp^{1}C$^{\alpha}H$	His^{2}N*H*	4.21	2.03	2.13 (0.07)
Trp^{1}C$^{\alpha}H$	His^{2}C$^{\alpha}H$	0.06	4.13	4.17 (0.08)
Trp^{1}C$^{\alpha}H$	His^{2}C$_2H$	0.10	3.79	3.78 (0.11)
His^{2}N*H*	His^{2}C$^{\alpha}H$	0.79	2.68	2.73 (0.06)
His^{2}N*H*	Trp^{3}N*H*	0.33	3.10	3.24 (0.06)
His^{2}C$^{\alpha}H$	Trp^{3}N*H*	4.85	1.98	2.21 (0.05)
His^{2}C$^{\alpha}H$	Trp^{3}C$_4H$	0.06	4.13	4.28 (0.08)
Trp^{3}C$^{\alpha}H$	His^{2}C$_4H$	0.32	3.12	3.11 (0.07)
Trp^{3}C$^{\alpha}H$	Trp^{3}N*H*	1.15	2.52	2.76 (0.04)
Trp^{3}N*H*	Leu^{4}N*H*	0.74	2.71	2.83 (0.07)
Trp^{3}C$^{\alpha}H$	Leu^{4}N*H*	5.51	1.94	2.04 (0.06)
Trp^{3}C$^{\alpha}H$	Leu^{4}C$^{\alpha}H$	0.16	3.51	3.70 (0.06)
Leu^{4}C$^{\alpha}H$	Gln^{5}N*H*	6.12	1.90	2.07 (0.05)
Leu^{4}C$^{\alpha}H$	Leu^{4}N*H*	0.99	2.58	2.73 (0.04)
Leu^{4}N*H*	Gln^{5}N*H*	0.79	2.68	2.77 (0.08)
Gln^{5}C$^{\alpha}H$	Gln^{5}N*H*	1.55	2.40	2.67 (0.04)
Gln^{5}N*H*	Leu^{6}N*H*	1.09	2.54	2.69 (0.06)
Lys^{7}N*H*	γ-lactam^{8}N*H*	0.65	2.77	2.77 (0.10)
Gly^{9}C$^{\alpha}H$	Gln^{10}N*H*	2.07	2.28	2.39 (0.12)
Gly^{9}C$^{\alpha'}H$	Gln^{10}N*H*	1.02	2.57	2.83 (0.06)
Gln^{10}C$^{\alpha}H$	Gln^{10}N*H*	0.93	2.61	2.75 (0.06)
Pro^{11}C$^{\alpha}H$	Nle^{12}N*H*	4.84	1.98	2.04 (0.05)
Nle^{12}C$^{\alpha}H$	Nle^{12}N*H*	1.85	2.33	2.26 (0.10)
Nle^{12}C$^{\alpha}H$	Tyr^{13}N*H*	3.69	2.07	2.13 (0.07)
Trp^{1}C$^{\beta}H$	His^{2}C$_2H$	0.80	2.69	2.72 (0.07)
Trp^{1}C$^{\beta'}H$	His^{2}C$_2H$	0.45	2.95	2.97 (0.11)
His^{2}C$_4H$	Trp^{3}C$^{\beta}H$	0.69	2.74	2.63 (0.09)
His^{2}C$_4H$	Trp^{3}C$^{\beta'}H$	0.38	3.00	3.09 (0.08)
Gly^{9}C$^{\alpha}H$	γ-lactam^{8}C$^{\gamma}H$	0.51	2.89	2.88 (0.11)
Gly^{9}C$^{\alpha'}H$	γ-lactam^{8}C$^{\gamma}H$	0.71	2.73	2.73 (0.12)
γ-lactam^{8}C$^{\gamma}H$	Gln^{10}N*H*	0.19	3.39	3.38 (0.10)
Gln^{10}C$^{\alpha}H$	Pro^{11}C$^{\delta}H$	1.28	2.48	2.78 (0.18)
γ-lactam^{8}C$^{\beta}H$	γ-lactam^{8}C$^{\beta'}H$	9.59	1.77	standard

[a] Experimental data are extracted from a NOESY spectrum (250 ms) in DMSO-d_6. [b] Calculated interproton distances are computed from 120 ps MD trajectories in DMSO and rmsd values of the 2000 structures obtained during dynamics are given in parentheses.

Strains and Media. The *Saccharomyces cerevisiae* strains used were *S. cerevisiae* RC629 [*MAT***a** *bar1-1* (supersensitive to α-factor due to mutation in the *BAR1* protease, allelic to *sst1*)] from R. Chan, University of Cincinnati, used in the biological response "halo" assay(*36*), *S. cerevisiae* DK102 (*MAT***a** *ura3-52 lys2-801 ade2-101 trp1-*Δ*63 his3-*Δ*280 leu2-*

Δ*1 ste2*::*HIS3 sst1*-Δ*5* with plasmid pNED1/*STE2*) was used in the binding competition assay (*37*), and *S. cerevisiae* LM23-3az [*MAT***a** *FUS1::lacZ bar1-1*] from Lorraine Marsh, Albert Einstein College of Medicine, New York, used to measure a pheromone-inducible gene (*38*).

For the binding competition assay, cells were grown in YM-1 medium (0.5% yeast extract, 1% peptone, 1% succinic acid, 0.6% NaOH, 1% dextrose, 0.67% yeast nitrogen base without amino acids, 0.001% uracil, and 0.001% adenine sulfate). All peptide dilutions, washes, and reaction incubations were carried out in YM-1 inhibitor (YM-1i) medium (YM-1 medium with 0.065% sodium azide, 0.1% KF, and 0.4% TAME added). YM-1i medium was filtered through a 0.2 mm filter (Gelman Sciences VacuCap 90) and chilled on ice prior to use. For the growth arrest (halo) and gene induction assays, cells were grown in YEPD broth (1% yeast extract, 2% peptone, and 2% dextrose). The biological activities of the pheromones in different assays (growth arrest and gene induction as described below) gave essentially identical results using the various strains. Thus, because there are not significant strain effects influencing these bioassays, comparisons can be made of various analogue activities as measured in different strains. All strains tested lacked the Bar1p protease that cleaves α-factor, and in previous investigations we showed that Bar1p protease-deficient strains do not cleave α-factor (*12*).

Growth Arrest (Halo) Assay. YEPD plates [yeast extract (1%, w/v), peptone (1% w/v), dextrose (2% w/v), and agar (2% w/v)] were overlaid with 4 mL of *S. cerevisiae* RC629 cells (2.5×10^5 cells/mL) in Noble agar. Filter disks (sterile blanks from Difco), 8 mm in diameter, were placed on the overlay, and 10 μL portions of peptide solutions at various concentrations were placed on the disks and formation of clear zones (halos) of growth arrest determined as previously described (*12*). [Nle^{12}]-α-Factor, an isosteric analogue that is equally as active as the wild-type pheromone (*39*), was used as a control in all bioactivity assays and in receptor binding. Differences in diffusion of the various analogues in the agar medium did not contribute to the differences in the biological activities in the halo assay. Similar trends were obtained for these analogues when activities were ranked within an assay as measured by the halo or gene induction assay (see below). In the latter assay, cells were suspended in liquid medium and diffusion through agar played no role in the activity of the soluble pheromones. Further evidence that diffusion rates do not determine bioactivity in the halo assay is given by the fact that there is no correlation between bioactivity and peptide hydrophobicity as measured by K' values on HPLC columns.

Effect of α-Factor Analogues on Gene Induction. S. cerevisiae LM23-3az carries a *FUS1* gene, which is inducible by mating pheromone, that is fused to the gene encoding β-galactosidase as a reporter. Cells were grown overnight in YEPD medium at 30 °C to 5×10^6 cells/mL, washed by centrifugation, and grown for one doubling at 30 °C. Induction was performed by adding 0.5 mL of peptide at various concentrations to 4.5 mL of concentrated cells (1×10^8 cells/mL). The suspensions were vortexed and placed at 30 °C with shaking for 2 h. After this time, cells were harvested by centrifugation, each pellet was resuspended, and assays were done for β-galactosidase in triplicate by a recently modified (*40*) standard protocol (*41*, *42*). The above experiments were done at least twice for each analogue, with the values plotted representing an average of these determinations.

Antagonism and Synergism Assays. Two assays were used to measure whether analogues that had no growth arrest activity by themselves were capable of antagonizing (interferring with activity by agonists) or synergizing (enhancing activity of agonists) activity of [Nle^{12}]-α-factor. In one assay, lawns of RC629 were overlaid onto YEPD plates as described in the growth arrest assay. Sterile disks were placed adjacent to each other so that the disk containing the test peptide would lie at the periphery of the halo formed by [Nle^{12}]-α-factor. One disk was impregnated with 1 μg of [Nle^{12}]-α-factor in 10 μL of H_2O, and the other disk was impregnated with various amounts of the test peptide in 10 μL of H_2O. Plates were incubated as described in the growth arrest assay and the effects on halo formation were noted.

A second assay for synergism/antagonism measured the propensity of a pheromone to induce changes in cell morphology. Strain RC629 was grown at 30 °C to 1×10^6 cells/mL in YEPD. Ninety microliters of cells was aliquoted into wells of a 96-well microtiter plate (Corning, round-bottom). To each well was added 10 μL of different concentrations of [Nle^{12}]-α-factor or analogues, and the suspension was incubated at 30 °C with shaking (200 rpm). Peptide concentrations tested were 5.0, 1.0, 0.5, 0.1, 0.08, 0.05, and 0.01 μg/mL. This assay was used to determine whether analogues inactive by themselves could increase or decrease morphogenesis induced by α-factor alone. Cells were incubated with increasing amounts of α-factor only or with α-factor plus the addition of analogue **5** or **6** at 10 μg/mL. Fifteen microliters of 37% formaldehyde (Sigma) was added to each well at the indicated times to fix the cell morphology. Total cells and total number of cells with shmoo morphology (an elongated, pear-shaped cell without a constricted neck at the bud site) were counted by visual inspection using a microscope (Leitz) under 320× power. The percentage of shmoos was calculated by dividing total shmooing cells by total cells (×100). Measurement of morphogenesis induced by each peptide was repeated at least twice, with the data obtained in duplicate experiments giving nearly identical results.

Binding Competition Assay. This assay was performed with membranes of strain DK102(pNED1) and HPLC-purified [^{3}H]-[Nle^{12}]-α-factor as described previously (*43*). Synthetic [^{3}H]-[Nle^{12}]-α-factor was labeled by reduction of dehydroproline containing α-factor by the TR3 hydrogenation procedure of Amersham International and purified by HPLC as described elsewhere (*39*). Binding of labeled α-factor to filters in the absence of membranes was less than 20 cpm. Specific binding is defined as (mean bound cpm/total mean cpm) × 100. Mean bound cpm is the average of 4 determinations for each binding point for each analogue and total mean cpm is the average of 4 determinations of the total counts incubated with each analogue. Results for each analogue were expressed as a percent of total binding in the absence of the analogue. Each binding assay was carried out at least two times with virtually identical curves obtained. The K_i values were calculated by dividing the experimentally determined concentration giving 50% binding displacement by $[1 + H_T/K_D]$, where H_T = concentration of radiolabel and K_D = dissociation constant of radiolabel (*44*).

RESULTS

Synthesis of γ-Lactam Peptidomimetic Building Blocks. The protected γ-lactams, 3-(*S*)-(*tert*-butoxycarbonyl)amino-2-oxo-1-pyrrolidineacetic acid (**1**) and 3-(*R*)-(*tert*-butoxycarbonyl)amino-2-oxo-1-pyrrolidineacetic acid (**2**) (Figure 1), required for preparation of the α-factor peptidomimetics were initially prepared from their respective Boc-Met-Gly-OMe *S*-methylsulfonium iodides following the literature procedure (*22*). However, we only obtained a 35% yield of the desired free acid due to incomplete hydrolysis of the corresponding methyl esters under the *in situ* hydrolysis conditions specified. This problem was rectified by a rapid posthydrolysis reaction effected by stirring the crude mixture in a medium-strength basic solution (pH = 12) for 5 min. This treatment plus a subsequent DCM washing at pH 8.5 raised the purity of the crude acid substantially. We also noted that, as indicated by ^{1}H NMR and FAB-MS (data not shown), extraction at pH 4.0 resulted in the loss of a large quantity of the product (∼40%) in the aqueous phase as its sodium salt. Complete recovery was obtained by use of cold 1 M HCl in the presence of ethyl acetate to reduce the pH to 2.5 for all acidifications. Using the above modifications, we obtained over 85% yield of a crystalline product that was homogeneous and characterized by proton NMR spectroscopy (see Experimental Procedures).

Solid-Phase Synthesis of Constrained Analogues of α-Factor. The solid-phase syntheses of α-factor analogues **3**, **4**, **5**, and **6** were carried out manually with the Boc/Bzl protecting strategy. The starting Boc-L-Tyr(*t*-Bu)−PAM resin (0.3 mmol) was elongated to give BocGlnProNleTyr-(*t*-Bu)−PAM resin, at which point the resin was split into smaller portions (∼0.1 mmol/portion) for divergently assembling all γ-lactam-containing analogues except des-Met^{12}-Tyr^{13}-[(*R*)-γ-lactam^{8,9}]-α-factor (**6**). In the latter case a Boc-Pro−PAM resin was utilized. The incorporation of the Boc-protected lactam "dipeptides", **1** and **2,** was accomplished by DIPC/HOBt coupling with 3 equiv of **1** or **2** in a mixture of DMF and DCM (1:10). During the coupling period, DIEA (ca. 0.1 mL) was added to the reaction vessel to maintain a weakly basic pH and the coupling was continued for 2 h until completeness was indicated by the Kaiser test (*45*). Syntheses of analogues containing *N*-methyl-L-alanine or sarcosine were carried out using standard procedures starting with *N*-α-FmocTyr(OtBu)−Wang resin. All purified peptides were greater than 99% homogeneous as judged by analytical HPLC and high-performance capillary electrophoresis (see Experimental Procedures). The HPLC analysis of the analogues indicated that these were devoid of measurable quantities of [Nle^{12}]-α-factor. Amino acid analysis of the synthetic peptides gave ratios generally within 15% of expected values, and FAB-MS determinations gave monoisotopic mass values within 0.4 amu of calculated values (data not shown). The presence of Trp residues was confirmed by measuring the ultraviolet absorption at 289 nm. The primary sequence of peptide **4** was confirmed by high-resolution NMR spectroscopy (vide infra).

Assignments of Amino Acid Spin Systems. Complete proton resonance assignments of all residues of [(*R*)-γ-lactam^{8,9}, Nle^{12}]-α-factor (**4**) were accomplished by use of one- and two-dimensional NMR spectroscopy (Table 1). DQF-COSY, HMQC, TOCSY, and HMQC-TOCSY were used to identify different spin systems of the peptide pheromone. The spin systems of Trp, His, and Tyr residues were differentiated from nonaromatic residues by their characteristic downfield C$^{\beta}$Hs (2.8−3.2 ppm). Upfield resonances, C$^{\delta}$Hs and C$^{\epsilon}$Hs (0.81−0.87 ppm), were used to recognize Leu and Nle residues, respectively. Side-chain resonances that do not show connectivities in DQF-COSY and TOCSY viz His^2 C_2H and C_4H, Gln^5 γNH$_2$ and Gln^{10} γNH$_2$, were assigned by analysis of the one-dimensional proton spectrum and intraresidue NOE connectivities. Replicated spin systems were distinguished by means of sequential NOEs. Carbon chemical shifts and intraresidue NOE connectivities were used to discriminate aromatic protons of Trp^1, Trp^3, and Tyr^{13} residues. The complete assignment of all resonances confirmed the composition of this peptide. 3-(*R*)-Acetamido-2-oxo-1-pyrrolidineacetamide (**7**) proton resonances were assigned from its DQF-COSY and TOCSY spectra (see Experimental Procedures).

Temperature Coefficients of Amide NHs and $^3J_{NH-C^{\alpha}H}$ Coupling Constants. Temperature dependencies of the backbone amide proton chemical shifts of [(*R*)-γ-lactam^{8,9}, Nle^{12}]-α-factor (**4**) were measured in order to assess intramolecular H-bonding or solvent exposure of the amide N*H*s. Small temperature coefficients reflect greater shielding from solvent and indicate possible involvement in strong intramolecular H-bonding. A temperature coefficient of 6 ppb/K or higher is expected for random coil structures and ≤5 ppb/K for solvent-shielded protons (*46*). All the amide N*H*s showed relatively high temperature coefficients, indicating a flexible conformation for this peptide. Among the 13 residues the Trp^3 amide N*H* had the lowest temperature coefficient (4.22 ppb/K). The His^2, Gln^5, Leu^6, Lys^7, Gln^{10}, and Nle^{12} amide NH protons had dδ/dT values of ∼5 ppb/K.

Vicinal proton coupling constants ($^3J_{NH-C^{\alpha}H}$) were extracted from a well-digitized one-dimensional proton spectrum of [(*R*)-γ-lactam^{8,9}, Nle^{12}]-α-factor (**4**). The coupling constants could not be measured for Leu^6, Lys^7, and Nle^{12} due to signal overlap and for Leu^4 because of poor resolution of its N*H* signal. The coupling constants were on the order of 7−8 Hz. Such values are generally associated with a population of structures representative of a flexible peptide (*47*, *48*).

NOESY Connectivities. Quantitative information on interproton distances for the structure determination of [(*R*)-γ-lactam^{8,9}, Nle^{12}]-α-factor (**4**) was obtained from the analysis of a NOESY spectrum measured on a DMSO-d_6 solution. DMSO-d_6 rather than water was chosen for the NMR analysis because the increased viscosity of DMSO affects the correlation times of linear peptides (*49*) and because it is easy to avoid interference by solvent peaks in this organic solvent. In previous studies on α-factor, much stronger cross-peaks were found in DMSO-d_6 than in water. Extensive NMR analyses on α-factor and α-factor analogues in DMSO-d_6 (*50, 51*) concluded that these pheromones assume a transient β-turn in this solvent. Most significantly, comparative studies in water indicated that α-factor assumed similar structures in both solvents. Given this observation, we elected to use DMSO-d_6 in the present study. Peak volumes were integrated on both sides of the diagonal and averaged. By assuming isotropic mobility and the isolated two-spin approximation (*52*), the observed average integrals

from a 250 ms mixing time NOESY spectrum were converted to interproton distances (Table 2). In cases where both methylene protons resonated at the same chemical shift, the observed NOESY cross-peak volume (I) has been corrected by using the formula $I_{cor} = {}^2/_3 I_{obs}$. The obtained distances were calibrated with respect to the distance between the β-methylene protons of the pyrrolidinone ring (1.77 Å). Both intra- and interresidue NOEs were detected in the molecule. [(*R*)-γ-Lactam[8,9], Nle[12]]-α-factor (**4**) adopts a trans configuration with respect to the Gln[10]−Pro[11] peptide bond as indicated by the characteristic NOE cross-peaks from the Gln[10] C$^{\alpha}H$ to the Pro[11] C$^{\delta}H$ (Table 2). Due to the absence of the $i + 2$ NH proton in [(*R*)-γ-lactam[8,9], Nle[12]]-α-factor (**4**), few NOESY cross-peaks characteristic of the turn region can be discerned. We did observe a cross-peak between the γ-protons of the 2-pyrrolidinone ring and the amide NH of Gln[10]. The distance between the latter protons was found to be 3.39 Å (Table 2). This distance is important in distinguishing different conformations for the center of the pheromone. A complete list of all NOESY-derived distances is given in Table 2.

Constrained Molecular Dynamics Calculations. The [(*R*)-γ-lactam[8,9],Nle[12]]-α-factor (**4**) was modeled with NMR-derived distance constraints (see Experimental Procedures). The average interproton distances obtained from the analysis of DMSO simulations (2000 structures) of this peptide are in very good agreement with their corresponding NOE-derived distances (a rmsd of less than 0.05 Å per distance, Table 2). The torsion angles (ϕ and ψ) of the 2000 structures obtained during the simulation in DMSO are shown in Ramachandran plots for γ-lactam ($i + 1$) and *N*-alkylated glycyl ($i + 2$) residues (Figure 2). The average dihedral angles ϕ_2, ψ_2, ϕ_3, and ψ_3 are 110°, 135°, 97°, and −50°, respectively.

CD Spectral Characteristics. The CD spectrum of [(*R*)-γ-lactam[8,9],Nle[12]]-α-factor (**4**) in Tris buffer is characterized by a weak trough at 240 nm, a positive ellipticity between 216 and 234 nm ($[\theta]_m = 18\,800$ deg·cm^2 dmol^{-1}) and a strong transition centered at 202 nm ($[\theta]_m = -46\,900$ deg·cm^2 dmol^{-1}) (Figure 3). 3-(*R*)-Acetamido-2-oxo-1-pyrrolidineacetamide (**7**) in Tris buffer exhibited a CD curve with a weak Cotton effect at 238 nm and a broad positive peak centered at 206 nm (Figure 3). The CD curve for an equimolar mixture of [Nle[12]]-α-factor and [(*R*)-γ-lactam]-dipeptide **7** in Tris buffer is qualitatively similar to that of [(*R*)-γ-lactam[8,9], Nle[12]]-α-factor in Tris buffer (Figure 3).

Activity of γ-Lactam Constrained Analogues of α-Factor in a Growth Arrest (Halo) Assay. The activity of the constrained analogues was judged by a growth arrest assay on agar plates. Zones of inhibition were measured and plotted versus the amount of peptide on a disk. The data were linearized by regression analysis and the amount of peptide that caused a 20 mm zone of growth inhibition was determined. All assays were run in duplicate and the results were reproducible within 10%. The results show that [(*S*)-γ-lactam[8,9], Nle[12]]-α-factor (**3**) was about 50% less active than [Nle[12]]-α-factor in this assay (Table 3). [(*R*)-γ-Lactam[8,9], Nle[12]]-α-factor (**4**) was equally active with the control [Nle[12]]-α-factor. Neither of the undecapeptide analogues, **5** and **6,** was even a weak agonist in this assay as indicated by their lack of effect on growth arrest (Table 3). Their inactivity is shown by the absence of a halo surrounding the disks impregnated with these analogues assayed by the growth arrest assay. However, the *N*-terminal

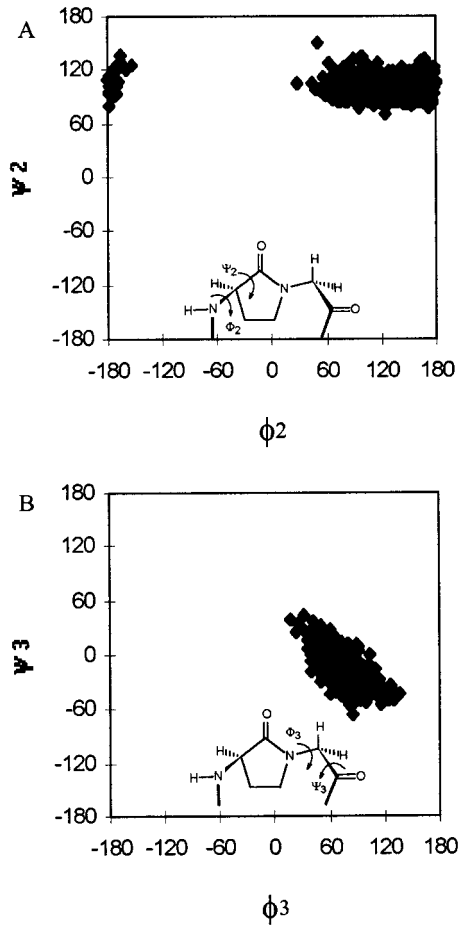

FIGURE 2: Ramachandran plots of the backbone torsion angles of the turn region of [(*R*)-γ-lactam[8,9], Nle[12]]-α-factor (**4**): (A) ϕ_2−ψ_2, (B) ϕ_3−ψ_3. Dihedral angles from 2000 conformers observed during a 120 ps molecular dynamics simulation in DMSO are included in the plot. The dihedral angles in panels A and B are those defined in the structure that has been superposed on the plot.

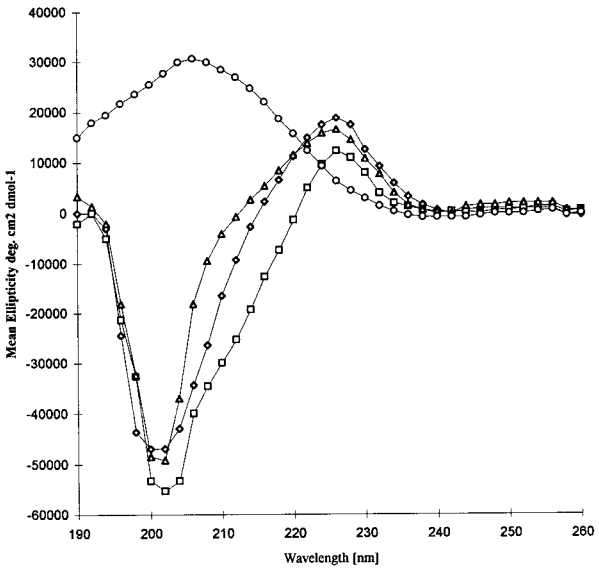

FIGURE 3: Circular dichroism measurement of [Nle[12]]-α-factor and analogues: (□) [Nle[12]]-α-factor, (◇) peptide **4**, (○) peptide **7**, and (△) an equimolar mixture of [Nle[12]]-α-factor and peptide **7**. All measurements were made in Tris buffer (50 mM, pH 7.2). The peptide concentration was approximately 0.5 mM.

Table 3: Bioactivity and Receptor Binding of [Nle[12]]-α-Factor and Analogues

peptide	halo[a]	LacZ[b]	binding[c]
WHWLGLKPGQP[Nle]Y[d]	1.0 ± 0.1	1.0 ± 0.2	1 ± 0.12
WHWLQLK[(*S*)-γ-lactam]QP[Nle]Y (**3**)	0.4 ± 0.03	0.7 ± 0.03	33 ± 2.4
WHWLQLK[(*R*)-γ-lactam]QP[Nle]Y (**4**)	1.0 ± 0.1	0.9 ± 0.1	4.5 ± 0.22
WLQLK[(*R*)-γ-lactam]QP[Nle]Y (**5**)	inactive	inactive	100 ± 9
WHWLQLK[(*R*)-γ-lactam]QP (**6**)	inactive	inactive	>5,000
WHWLQLK-D-PGQP[Nle]Y	0.3 ± 0.02	0.4 ± 0.07	125 ± 8.6
WHWLQLKP[Sar]QP[Nle]Y	1.4 ± 0.1	1.1 ± 0.3	1.3 ± 0.33
WHWLQLKP[Me-D-Ala]QP[Nle]Y	1.3 ± 0.1	1.3 ± 0.2	0.6 ± 0.05

[a] Activity relative (± standard error of the mean) of [Nle[12]]-α-factor needed to cause a halo of 20 mm within 24 h. For [Nle[12]]-α-factor, 1.3 μg was required. [b] Amount of β-galactosidase activity (± standard error of the mean) induced by analogues (50nM) relative to that produced by [Nle[12]]-α-factor at 50 nM. [c] The dissociation constant (± standard error of the mean) relative to that of [Nle[12]]-α-factor determined by the displacement of [^{3}H][Nle[12]]-α-factor from the receptor as calculated according to Linden (*44*). For [Nle[12]]-α-factor the K_d was 2.0×10^{-8} M. A value greater than 1.0 indicates lower affinity. [d] An isosteric analogue of wild-type α-factor used as a control in all bioassays.

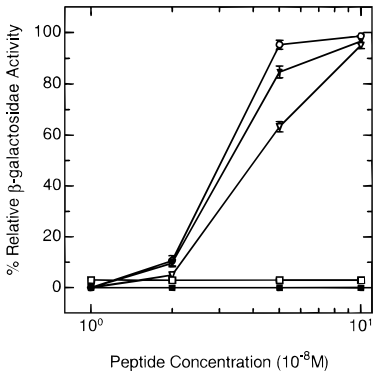

FIGURE 4: Gene induction (*FUS1−LacZ*) induced by [Nle[12]]-α-factor and various analogues. β-Galactosidase was measured in cultures incubated at various concentrations of peptide as shown: [Nle[12]]-α-factor (○), peptide **3** (▽), peptide **4** (▼), peptide **5** (□), and peptide **6** (■).

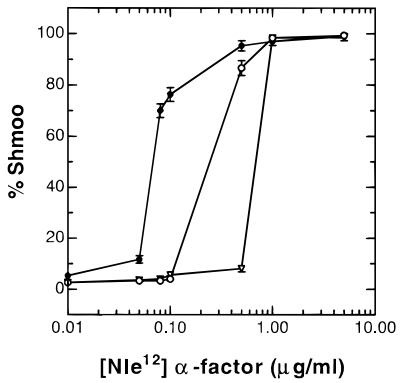

FIGURE 5: Morphogenesis induced by [Nle[12]]-α-factor with and without analogues **5** and **6**. Cellular morphogenesis at various concentrations of α-factor is shown with α-factor alone (○), α-factor plus 10 μg/mL analogue **5** (▽), and α-factor plus 10 μg/mL analogue **6** (●).

truncation (**5**) leads to antagonism of the activity of [Nle[12]]-α-factor while the *C*-terminal truncation (**6**) actually stimulates the activity of this pheromone. Increasing amounts of **5** lead to an inhibition of the growth arrest by [Nle[12]]-α-factor as noted by the decrease in the halo juxtaposed to the disk impregnated with **5** (data not shown). In contrast, increasing amounts of **6** lead to an enhancement of growth arrest by the pheromone as noted by the increase in the halo juxtaposed to the disk with **6** (data not shown).

Biological Activity of γ-Lactam Constrained Analogues of α-Factor in Solution. The halo assay is carried out in agar and may reflect effects of diffusion as well as the inherent biological activity of the various α-factor analogues. To gain further insights into the peptidomimetic analogues, we also assayed their biological activities in solution. The yeast mating pheromones activate the transcription of several genes such as *FUS1*, which are critical for signal transduction. This assay is carried out with cells suspended in culture medium by determining the production of β-galactosidase as a reporter of *FUS1* in response to various amounts of peptide (see Experimental Procedures). [(*R*)-γ-Lactam[8,9], Nle[12]]-α-factor (**4**) exhibited potency comparable to that of the wild-type pheromone in the *FUS1−lacZ* assay (Table 3, Figure 4). The (*S*)-γ-lactam[8,9] homologue (**3**) was slightly less active than either its (*R*)-γ-lactam[8,9] homologue (**4**) or [Nle[12]]-α-factor. Neither of the truncated analogues (**5, 6**) was active up to a concentration of 10^{-6} M.

α-Factor causes *MAT***a** cells to change shape when a suspension of cells is challenged with pheromone. Interestingly, both constrained tridecapeptides **3** and **4** were as active as [Nle[12]]-α-factor in the morphogenesis assay (data not shown). Neither the N-terminal-truncated analogue **5** nor the C-terminal-truncated undecapeptide **6** caused *MAT***a** cells to change shape at the highest concentrations examined (20 μg/mL; >300-fold less active than [Nle[12]]-α-factor). However, in the presence of analogue **5**, more α-factor was required to induce morphogenesis, whereas addition of analogue **6** together with α-factor caused induction of morphogenesis at lower α-factor concentrations (Figure 5). This assay, therefore, confirms the antagonistic and synergistic characteristics of **5** and **6,** respectively.

Binding of γ-Lactam Constrained Analogues to the α-Factor Receptor. The affinities of the constrained analogues for the α-factor receptor (Ste2p) were assessed by determining their ability to displace tritiated [Nle[12]]-α-factor from the receptor. The displacement curves are reasonably parallel to that of [Nle[12]]-α-factor and the avidity of the different compounds can be compared by the amount of peptide that displaced 50% of the tritiated peptide from the receptor (Figure 6 and Table 3). [(*R*)-γ-Lactam[8,9], Nle[12]]-α-factor exhibited a 4.5-fold higher K_i than that of the [Nle[12]]-α-factor in the receptor binding assay. A greater affinity drop was observed for the diastereomeric analogue **3**, which bound about 33-fold less effectively than the [Nle[12]]-α-factor. We and other investigators have shown that there is not always a close correlation between biological activity of α-factor analogues and their binding to the receptor (*12*, *13*, *38*). This has been attributed to the

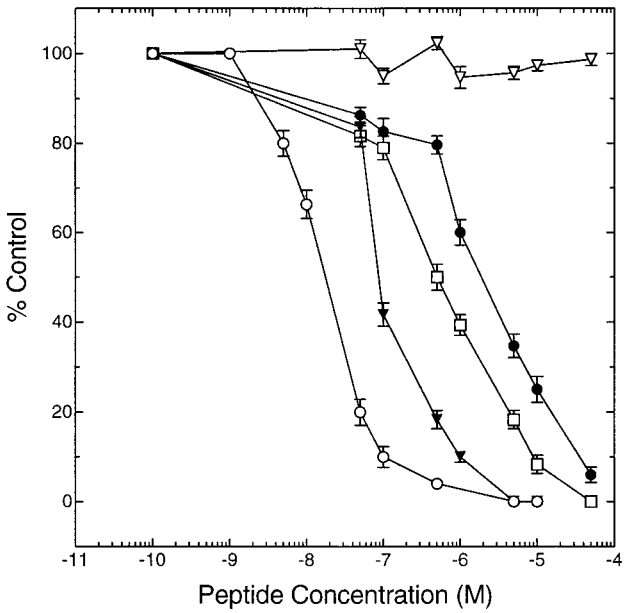

FIGURE 6: Competition binding assays. Binding of the analogues was performed in competition with [^{3}H]-α-factor. The binding curves are for [Nle^{12}]-α-factor (○), analogue **4** (▼), analogue **3** (□), analogue **5** (●), and analogue **6** (▽).

differences in the amount of time for the biological response to be measured in comparison to the time required to determine the binding constant and to different response pathways with various thresholds that may be triggered by pheromone binding. The N-terminal-truncated analogue **5** bound with approximately 20-fold lower affinity than the full-length constrained tridecapeptide containing the identical γ-lactam (**4**). The synergist (**6**) had no measurable affinity for the receptor up to a concentration of 10^{-4} M.

Biological Activities of Other Constrained Analogues. The biological activities and receptor binding affinities were determined for [D-Pro^8,Nle^{12}]-α-factor, [Sar^9,Nle^{12}]-α-factor and [Me-D-Ala^9,Nle^{12}]-α-factor. [D-Pro^8,Nle^{12}]-α-factor exhibited low activities in both the growth arrest and gene induction assays and had less than 1% the receptor affinity of [Nle^{12}]-α-factor. In contrast, both of the peptides with *N*-methyl residues in position 9 were slightly more active than [Nle^{12}]-α-factor in the growth arrest and gene induction assays and bound to the α-factor receptor as strongly as the native pheromone (Table 3).

DISCUSSION

Reverse turn folding motifs have been found as biologically relevant secondary structural components in numerous peptide hormones (*23*, *45*, *53*). In principle, structural restriction in a peptide hormone by means of reducing conformational flexibility at the turn region should lead to an enhanced biological activity (*54*). Using various strategies to attain conformational constraints, significant increases in peptide potency were obtained for somatostatin (*55, 56*), α-melanocyte-stimulating hormone (*57*), luteinizing hormone-releasing hormone (*18*, *58*, *59*), and α-amylase inhibitor (*60*). These constraints include interresidue cyclization, incorporation of sterically hindered unnatural amino acids, or the use of peptidomimetic building blocks. In recent years the number of peptidomimetics found to restrict local conformations have proliferated extensively (for reviews see refs *61* and *62*).

We previously reported experimental data supporting the conclusion that α-factor adopted a transient β-turn secondary structure around Pro^8−Gly^9 in its biologically active conformation (*7*, *8*, *50*, *63*). In our laboratory several attempts have been made to constrain the turn region of α-factor. Lactamization via the side chains of Lys^7 and Glu^{10} resulted in agonists with only a tenth the activity and severely decreased receptor affinity compared to α-factor (*9*, *11*). Disulfide formation between sulfhydryl groups of Cys residues that had been inserted at positions 7 and 10 of α-factor resulted in an approximately 5−10-fold increase in activity compared to that of uncyclized homologue (*12*) and $^1/_{10}$ the activity of α-factor. No previous attempt at constraining the central turn region of the pheromone has resulted in peptides of activity equal to, or greater than, that of native α-factor.

Biological and Biochemical Ramifications of the γ-Lactam. In the present study we found that insertion of a peptidomimetic, the Freidinger's γ-lactam, in the turn region of α-factor resulted in peptides with high potency. Analogue **4** had a potency equal to that of α-factor in the halo, morphogenesis, and gene induction assays. This analogue represents, therefore, the first example of a peptidomimetic of the turn region of the mating pheromone with a potency equal to that of wild-type α-factor. It is interesting that compound **3**, which has (*S*)-chirality at the position 8 α-carbon, exhibited from 50% to 100% of the α-factor activity in the various assays. The major difference that one would predict for compounds **3** and **4** would be the type of turn that they assume.

Peptide pheromones **3** and **4** exhibited affinities for the α-factor receptor (Ste2p) that were 33-fold and 4.5-fold lower, respectively, than that of the control pheromone ([Nle^{12}]-α-factor). A peptide with D-*P*ro^8 had low biological activity and less than 1% the receptor affinity of the L-Pro^8 homologue ([Nle^{12}]-α-factor). In a recent study we found that replacement of Pro^8 with L-Ala resulted in an 11-fold decrease in receptor affinity, whereas insertion of D-Ala at this position caused a 300-fold drop in affinity (*13*). Peptide **3** has the L-configuration at the position 8 α-carbon, whereas peptide **4** has the inverse stereochemistry. Based on our findings on the influence of chirality of the α-carbon of the position 8 residue, the γ-lactam analogues of α-factor have receptor binding constants that are exactly opposite to those which would be predicted. We believe that this result indicates that the conformation assumed by the central region of the pheromone is strongly influenced by the γ-lactam moiety and that the conformation of this region affects the binding of these analogues to Ste2p.

The 3−13 peptide containing the γ-lactam (**5**) did not exhibit any biological activity, and this undecapeptide inhibited the potency of α-factor in the growth arrest assay. Therefore, it may be classified as an antagonist. The K_i value of **5** indicates that this 3−13 fragment of α-factor binds about 20-fold less avidly to the receptor than tridecapeptide **4**. In a previous study we found that desTrp^{1}desHis^2[Nle^{12}]-α-factor bound about 4-fold less effectively than [Nle^{12}]-α-factor to Ste2p (*64*). The 1−11 γ-lactam containing undecapeptide **6** was inactive in all bioassays and did not bind to the receptor at concentrations up to 10^{-4} M, yet it

potentiated the activity of the α-factor. Thus, this undecapeptide is a synergist in analogy with the 1−11 sequence of the wild-type pheromone (*65*). As shown previously (*65*), synergistic activity is not due to direct interaction between α-factor and synergist that might cause a change in conformation or stabilization in α-factor leading to greater apparent activity. The biochemical basis of synergist activity is not known and is currently under investigation in our lab. In conclusion, the γ-lactam moiety is compatible with agonistic, antagonistic, and synergistic properties previously described for analogues of the α-factor.

*Biophysical Analysis of [(R)-γ-Lactam^{8,9}, Nle^{12}]-α-factor (**4**).* Conformational analysis of the γ-lactam turn constraint was previously approached by using both spectroscopy and molecular modeling. It was shown by an X-ray diffraction study that in the crystal state a tripeptide amide containing the (*S*)-γ-lactam constraint in place of positions $i + 1$ and $i + 2$ adopts a conformation very close to an ideal type II′ β-turn (*20*). Similarly, on the basis of computerized molecular simulation and energy minimization, Freidinger reported that a constrained luteinizing hormone-releasing hormone analogue with a (*S*)-γ-lactam moiety in place of residues 6 and 7 adopted a type II′ β-turn conformation (*18*). An NMR line-broadening investigation supported this conformational analysis (*19*). The γ-lactam conformational constraint offers effective restriction of the dihedral angle ψ_2, −130° compared to −120° for the ideal type II′ β-turn (*20*). Nevertheless, a certain amount of conformational flexibility is expected for this type of γ-lactam structural motif as none of the other torsion angles is covalently fixed.

CD spectral studies on [(*R*)-γ-lactam^{8,9}, Nle^{12}]-α-factor (**4**) and appropriate controls were recorded in Tris buffer (Figure 4). Previous CD studies on α-factor suggested that this linear peptide is predominantly disordered in aqueous buffer (*50, 66)*. The CD curve of [(*R*)-γ-lactam^{8,9}, Nle^{12}]-α-factor is characterized by a very weak trough at 240 nm, a positive band at 215−235 nm, and a negative band centered at 202 nm. Such a curve would be associated with a predominantly unstructured peptide. The CD pattern of 3-(*R*)-acetamido-2-oxo-1-pyrrolidineacetamide (**7**), a model dipeptide that represents the loop region of the γ-lactam-containing α-factor, exhibited a weak minimum near 238 nm and a broad positive peak centered at 206 nm. Although there are differences in exact peak positions and intensities, the overall shape of this curve is similar to those calculated for β-turns (*65)* and found for $i \rightarrow i + 3$ cyclized model tetrapeptides containing β- and/or γ-turns (*67, 68*). The CD spectrum measured on an equimolar mixture of 3-(*R*)-acetamido-2-oxo-1-pyrrolidineacetamide (**7**) and [Nle^{12}]-α-factor is qualitatively very similar to that found for [(*R*)-γ-lactam^{8,9}, Nle^{12}]-α-factor (**4**). Hence, it is reasonable to assume that the central loop region of lactam-containing α-factor **4** retains the conformation assumed by the lactam-containing dipeptide. The presence of γ-lactam in the α-factor analogue results in an increase in the intensity of positive ellipticity and a slight decrease in width and intensity of negative ellipticity. Otherwise the spectrum is identical to that of [Nle^{12}]-α-factor in Tris buffer, indicating more or less similar conformational features in both peptide pheromones.

The results of the NMR analysis of [(*R*)-γ-lactam^{8,9}, Nle^{12}]-α-factor (**4**) suggest that the peptide is rather flexible. All coupling constants and temperature coefficients are consistent with an averaged structure and with a lack of significant H-bonding or solvent shielding. Nevertheless, the NOE analysis indicated that the distance between the γ-protons of the 2-pyrrolidinone ring and the amide N*H* of Gln^{10} is relatively short (3.39 Å). Since both of the γ-protons of the 2-pyrrolidinone ring resonated at the same chemical shift, we used the distance between the center of these methylenic γ-protons and the Gln^{10} amide N*H* to examine the turn conformation. In an extended structure this interproton distance should be long (4.6 Å). In the case of an ideal type II β-turn conformation about γ-lactam^{8,9} ($i + 1$, $i + 2$) it should be 3.1 Å, and it is calculated to be 3.7 Å (an intermediate value) for a γ-turn conformation. Thus, the experimental value suggests that the γ-lactam-containing α-factor analogue (**4**) is probably in a somewhat bent structure. This conclusion is supported by the molecular dynamics simulation (see below).

The constrained molecular dynamics simulation provided an ensemble of structures that gave average distances that were in good agreement with the NMR-derived distances (Table 2). Distances normally characteristic of a β-turn cannot be monitored in peptide **4** due to the absence of the $i + 2$ residue amide N*H*. Therefore, we used the virtual torsion angle, β, defined by the α-carbon atoms of residues i, $i + 1$, $i + 2$, and the N atom of the $i + 3$ residue (0° ± 30°), and the interatomic distance between the α-carbon atoms of the i and the $i + 3$ residue (<7 Å) to assess the backbone conformation in the γ-lactam region (*69*). The average virtual β-torsion angle (19°) and the $i-i + 3$ inter-α-carbon distance (7.4 Å) obtained from dynamics simulations indicate that the Lys^7−Gln^{10} fragment assumes a reverse turn conformation. The large H-bond distance from the carbonyl oxygen of residue i to the $i + 3$ residue amide N*H* (∼6 Å) rules out the presence of a moderate to strong H-bond between these atoms and suggests, therefore, a conformation that deviates from an idealized β-turn. The average dihedral angles ϕ_2, ψ_2, ϕ_3, and ψ_3 are 110°, 135°, 97°, and −50°, respectively. Torsion angles ψ_2 and ϕ_3 are close to ideal values for a type II β-turn (120° and 80°, respectively). However, it appears that the γ-lactam is not effective at constraining torsion angles ϕ_2 and ψ_3 in the range expected for a type II turn as these dihedral angles deviate markedly from the ideal values (−60° and 0°, respectively). This finding is consistent with the X-ray diffraction results on the (*R*)-γ-lactam PLG analogue (*20*), where ϕ_2 and ψ_3 were also not influenced by the lactam constraint ($\phi_2 = 118°$, $\psi_2 = 142°$, $\phi_3 = 79°$, and $\psi_3 = -144°$).

The Ramachandran map (Figure 2) reveals that the backbone in peptide **4** adopts a γ-turn around the glycyl residue most of the time during the dynamics simulation in DMSO. The average torsion angles ($\phi_3 = 97°$ and $\psi_3 = -50°$) are within ±15° of those for an ideal γ-turn (70° to 85° and −60 to −70°) (*69*). The H-bond between the Gln^{10}N*H* and the lactam's carbonyl oxygen repeatedly forms and breaks during the simulations in DMSO. Though the Gln^{10} N*H* temperature coefficient does not support significant H-bonding, there are reverse turn structures documented in the literature in which H-bonds do not result in low temperature coefficients (*70*). In summary, both the NMR and CD results are compatible with a relatively flexible structure for peptide **4** with NOEs supporting a turn in the middle of the pheromone.

The constrained MD analyses suggest that a transient γ-turn around the *N*-alkylated glycine residue in position 9 is the most likely structure for the turn region of this molecule. This observation was further tested to see how the simulation results are affected by not including the NOEs at all. All distance constraints were deleted from the NMR-compatible starting structure and unconstrained dynamic simulations were performed. In addition, to study the effect of the starting structure on the course of dynamics, we performed simulations on an extended structure of **4** (generated as explained in the Experimental Procedures section) under identical conditions. Interestingly, both additional simulations revealed that the peptide folds into a turn structure around the γ-lactam moiety. A seven-member H-bonded ring centered around *N*-alkylated glycyl residue closed by Glu N*H* and lactam CO repeatedly forms and breaks during the simulations, which is consistent with a transient γ-turn. This suggests that the covalent constraint of the γ-lactam ring is sufficient to induce a transient turn structure into this peptide pheromone from the perspective of molecular dynamics simulations. The only significant difference in the constrained dynamics was narrowing the range of the ψ_3 torsion angle.

Correlation of Peptide Conformation and Biological Activity. The biological activities manifested by the γ-lactam-containing α-factor analogues reflect their receptor affinity, their inherent potencies, and their stability in the biological assay. In the present study *S. cerevisiae* strains lacking the BAR1 protease were used in all bioassays. Furthermore, HPLC analysis of α-factor analogues incubated with Bar1$^-$ mutants of *S. cerevisiae* revealed that the peptides are not cleaved by the cells (*12*). These facts suggest that pheromone degradation would not influence the activities of these analogues. The active pheromones analyzed in this investigation are likely to all have some tendency to form turns in the middle of the peptide. Studies on α-factor containing the Pro-Gly sequence support a type II β-turn (*7*, *10*). The present analysis supports a transient γ-turn for analogue **4**. Since this latter peptide is slightly more active than [Nle^{12}]-α-factor and exhibited higher bioactivity than its diastereomeric homologue [(*S*)-γ-lactam^{8,9}, Nle^{12}]-α-factor (**3**) [which would be expected to assume a type II′ β-turn (*20*)], it appears that different turns in the center of α-factor analogues can be accommodated by the receptor but that the accompanying stereochemical differences will affect the potency and receptor affinity of the resulting pheromone. This conclusion is supported as well by the biological activities of the Sar^9-α-factor and the Me-D-Ala^9-α-factor. On the basis of theoretical calculations (*23*), these *N*-methylated peptides are predicted to have stablilized reverse turns. Given the results of the present paper and our findings with other constrained analogues of α-factor (*11*, *12*), it is clear that a variety of turns in the center of α-factor can be accommodated by the receptor with effects on both receptor affinity and pheromone potency. We believe that until the conformation of α-factor complexed to its receptor can be determined, one should avoid the decision that a β-turn is the biologically active structure. It is most prudent to conclude that the relatively high biological affinities and receptor affinities of the constrained analogues studied herein indicate that a turn or bend in the pheromone is necessary for a productive interaction of α-factor and its receptor.

In summary, the results reported in this paper represent the first example of a peptidomimetic analogue of α-factor with activity approximately equal to that of the native pheromone. As judged primarily by NMR and modeling analysis, insertion of the Freidinger's (*R*)-γ-lactam in place of residues 8 and 9 of [Nle^{12}]-α-factor leads to a relatively flexible molecule that exhibits a preference for a γ-turn-like structure in the center of the pheromone. Moreover, our results provide evidence that the Freidinger γ-lactam conformational constraint can be used to maintain the biological activity of linear peptide hormones. The peptidomimetics have provided new insights into the relationship between the structure, activity, and receptor affinity of the pheromone and are useful tools to unravel the molecular basis for α-factor activity.

ACKNOWLEDGMENT

We thank Dr. Thomas Strekas of Queens College, CUNY, for the use of the CD spectrometer.

REFERENCES

1. Sprague, G. F., Jr., and Thorner, J. W. (1992) Molecular and Cellular Biology of the Yeast *Saccharomyces*, in *Gene Expression* (Johns, E. W., Pringle, J. R., and Broach, J. R., Eds.) Vol. 2, pp 657−744, Cold Spring Harbor Laboratory Press, Cold Spring Harbor, NY.
2. Stotzler, D., Klitz, H., and Duntze, W. (1976) *Eur. J. Biochem. 69*, 397−400.
3. Anderegg, R. J., Betz, R., Carr, S. A., Crabb, J. W., and Duntze, W. (1988) *J. Biol. Chem. 263*, 18236−18240.
4. Dohlman, H. G., Thorner, J., Caron, M. G., and Lefkowitz, R. J. (1991) *Annu. Rev. Biochem. 60*, 653−688.
5. Watson, S., and Arkinstall, S. (1994) *The G-Protein Linked Receptor Facts Book*, Academic Press, London.
6. Gilman, A. G. (1995) *Angew. Chem., Int. Ed. Engl. 34*, 1406−1419; Rodbell, M. (1995) *Angew. Chem., Int. Ed. Engl. 34*, 1420−1428; Strader, C., Fong, T. M., Graziano, M. P., and Tota, M. R. (1995) *FASEB J. 9*, 745−754.
7. Jelicks, L. A., Naider, F., Shenbagamurthi, P., Becker, J. M., and Broido, M. S. (1988) *Biopolymers 27*, 431−449.
8. Gounarides, J. S., Broido, M. S., Becker, J. M., and Naider, F. (1993) *Biochemistry 32*, 908−917.
9. Xue, C.-B., Eriotou-Bargiota, E., Miller, D., Becker, J. M., and Naider, F. (1989) *J. Biol. Chem. 264*, 19161−19168.
10. Gounarides, J. S., Xue, C.-B., Becker, J. M., and Naider, F. (1994) *Biopolymers 34*, 709−720.
11. Yang, W., McKinney, A., Becker, J. M., and Naider, F. (1995) *Biochemistry 34*, 1308−1315.
12. Xue, C.-B., Mckinney, A., Lu, H.-F., Jiang, J., Becker, J. M., and Naider, F. (1996) *Int. J. Pept. Protein Res. 47*, 131−141.
13. Abel, M. G., Zhang, Y. L., Lu, H., Naider, F., and Becker, J. M. (1998) *J. Pept. Res*. (in press).
14. Nagai, U., Sato, K., Nakamura, R., and Kato, R. (1993) *Tetrahedron Lett. 49*, 3577−3592.
15. Lombart, H.-G., and Lubbell, W. D. (1994) *J. Org. Chem. 59*, 6147−6149.
16. Hinds, M. G., Richards, N. G. J., and Robinson, J. A. (1988) *J. Chem. Soc., Chem. Commun.*, 1447−1449.
17. Genin, M. J., and Johnson, R. L. (1992) *J. Am. Chem. Soc. 114*, 8778−8783.
18. Freidinger, R. M., Veber, D. F., Perlow, D. S., Brooks, J. R., and Saperstein, R. (1980) *Science, 240*, 656−658.
19. Kopple, K. D. (1981) *Peptides, Synthesis and Function* (Rich, D. H., and Gross, E., Eds.) pp 295−298, Pierce Chemical Co., Rockford, IL.
20. Valle, G., Crisma, M., Toniolo, C., Yu, K. L., and Johnson, R. L. (1989) *Int. J. Pept. Protein Res. 33*, 181−190.
21. Ede, N. J., Rae, I. D., and Hearn, M. T. W. (1994) *Int. J. Pept. Protein Res. 44*, 568−581.

22. Freidinger, R. M., Perlow, D. S., and Veber, D. F. (1982) *J. Org. Chem. 47*, 104−109.
23. Chalmers, D. K., and Marshall, G. R. (1995) *J. Am. Chem. Soc. 117*, 5927−5937.
24. .Perczel, A., Kollat, E., Hollosi, M., and Fasman, G. D. (1993) *Biopolymers 33*, 665−685.
25. Piantini, U., Sorensen, O. W., and Ernst, R. R. (1982) *J. Am Chem. Soc. 104*, 6800−6801.
26. Rance, M., Sorensen, O. W., Bodenhausen, G., Wagner, G., Ernst, R. R., and Wuthrich, K (1983) *Biochem. Biophys. Res. Commun. 117*, 458−479.
27. Braunschweiler, L, and Ernst, R. R. (1983) *J. Magn. Reson. 53*, 521−528.
28. Bax, A., Byrd, R. A., and Aszalos, A. (1984) *J. Am Chem. Soc. 106*, 7632−7633.
29. Bax, A., and Davis, D. G. (1985) *J. Magn. Reson. 65*, 355−360.
30. Jeener, J., Meier, B. H., Bachmann, P., and Ernst, R. R. (1979) *J. Chem. Phys. 71*, 4546−4533.
31. Muller, L. (1979) *J. Am Chem. Soc. 101*, 4481−4484.
32. Bax, A., Griffey, R. H., and Hawkins, L. B. (1983) *J. Magn. Reson. 55*, 301−331.
33. Lerner, A., and Bax, A. (1986) *J. Magn. Reson. 69*, 375−380.
34. States, D. J., Haberkorn, R. A., and Ruben, D. J. (1982) *J. Magn. Reson. 48*, 286−292.
35. Marepalli, H. R., Antohi, O., Becker, J. M., and Naider, F. (1996) *J. Am. Chem. Soc. 118*, 6531−6539.
36. Chan, R. K., and Otte, C. A. (1982) *Mol. Cell. Biol. 2*, 11−20.
37. Jenness, D. D., Burkholder, A. C., and Hartwell, L. H. (1986) *Mol. Cell. Biol. 6*, 318−320.
38. Marsh, L. (1992) *Mol. Cell. Biol. 12*, 3959−3966.
39. Raths, S. K., Naider, F., and Becker, J. M. (1988) *J. Biol. Chem. 263*, 17333−17341.
40. Kippert, F. (1995) *FEMS Microbiol. Lett. 128*, 201−206.
41. Guarente, L. (1983) *Methods Enzymol. 101*, 167−180.
42. Miller, J. H. (1975) *Experiments in Molecular Genetics*, Cold Spring Harbor Laboratory, Cold Spring Harbor, NY.
43. David, N. E., Gee, M., Ansersen, B., Naider, F., Thorner, J., and Stevens, R. C. (1997) *J. Biol. Chem. 272*, 15553−15561.
44. Linden, J. (1982) *J. Cyclic Nucleotide Res. 8*, 163−172.
45. Kaiser, E., Colescott, R. L., Bossinger, C. D., and Cook, P. I. (1970) *Anal. Biochem. 34*, 595−598.
46. Rose, G. D., Gierasch, L. M., and Smith, J. A. (1985) *Adv. Protein Chem. 37*, 1−107.
47. Karplus, M. J. (1959) *J. Chem. Phys. 30*, 11−15.
48. Bystrov, V. F. (1976) *Prog. Nucl. Magn. Reson. Spectrosc. 10*, 41−81.
49. Amodeo, P., Motta, A., Picone, D., Tancredi, T., and Temussi, P. A. (1991) *J. Magn. Reson. 95*, 201−201.
50. Jelicks, L. A., Broido, M. S., Becker, J. M., and Naider, F. (1989) *Biochemistry 28*, 4233−4240.
51. Gounarides, J. S., Broido, M. S., Becker, J. M., and Naider, F. R. (1993) *Biochem. 32*, 908−917.
52. Neuhaus, D., and Williamson, M. (1989)*The Nuclear Overhauser Effect in Structural and Conformational Analysis*, VCH, Weinheim, Germany.
53. Marshall, G. R. (1992) *Curr. Opin. Struct. Biol. 2*, 904−919.
54. Hruby, V. J. (1982) *Life Sci. 31*, 189−199.
55. Arison, B. H., Hirschmann, R., and Veber, D. F. (1978) *Bioorg. Khim. 7*, 447−451.
56. Brady, S. F., Paleveda, W. J. Jr., Arison, B. H., Saperstein, R., Brady, E. J., Raynor, K., Reisine, T., Veber, D. F., and Freidinger, R. M. (1993) *Tetrahedron 49*, 3449−3466.
57. Sawyer, T. K., Cody, W. L., Knittle, J. J., Hruby, V. J., Hadley, M. E., Hirsh, M. D., and O'Donohue, T. L. (1983) in *Peptides: Structure and Function*, Proceedings of the 7th American Peptide Symposium (Hruby, V. J., and Rich, D. H., Eds.) pp 323−331, Pierce Chemical Co., Rockford, IL.
58. Monahan, M. W., Amoss, M. S., Anderson, H. A., and Vale, W. (1973) *Biochemistry 12*, 4616−4620.
59. Ling, N., and Vale, W. (1975) *Biochem. Biophys. Res. Commun. 63*, 801−805.
60. Etzkorn, F. A., Guo, T., Lipton, M., Goldberg, S. D., and Bartlett, P. A. (1994) *J. Am. Chem. Soc. 116*, 10412−10425.
61. Olson, G. L., et al. (1993) *J. Med. Chem. 36*, 3039−3049.
62. Gante, J. (1994) *Angew. Chem., Int. Ed. Engl. 33*, 1699−1720.
63. Naider, F., Gounarides, J. S., Xue, C.-B., Bargiota, E., and Becker, J. M. (1992) *Biopolymers 32*, 335−339.
64. Shenbargamurthi, P., Kundu, B., Raths, S., Becker, J. M., and Naider, F. (1985) *Biochemistry 24*, 7070−7076.
65. Eriotou-Bargiota, E., Xue, C.-B., Naider, F., and Becker, J. M. (1992) *Bichemistry 31*, 551−557.
66. Higashijima, T., Fujimura, K., Masui, Y., Sakakibara, S., and Miyazawa, T. (1983) *FEBS Lett. 159*, 229−232.
67. Woody, R. W. (1974) in *Peptides, Polypeptides and Proteins* (Blout, E. R., Bovey, F. A., Goodman, M., and Lotan, N. Eds.) pp 338−350, Wiley-Interscience, New York.
68. Rao, M. H., Yang, W., Joshua, H., Becker, J. M., and Naider, F. (1995) *Int. J. Pept. Protein Res. 45*, 418−429.
69. Nemethy, G., and Printz, M. P. (1972) *Macromolecules 5*, 755−758.
70. Von Dreele, P. H., Rae, I. D., and Scheraga, H. A. (1978) *Biochemistry 17*, 956−962.

BI980787U